

Constructing constitutive strength relationships for seismic and aseismic faulting

N. M. Beeler, U. S. Geological Survey, Menlo Park, California, 94025

Cascades Observatory, Vancouver, Washington, 98683

Brown University, Providence, Rhode Island, 027012

0. Abstract

For the purpose of modeling natural fault slip, a useful result from an experimental fault mechanics study would be a physically-based constitutive relation that well characterizes all the relevant observations. This report describes an approach for constructing such equations to represent laboratory or field observations. Where possible the construction intends to identify or, at least, attribute physical processes and contact scale physics to the observations such that the resulting relations can be extrapolated from laboratory conditions and scales to the Earth. The approach is developed in the context of *Ruina* [1983] and is illustrated initially by re-deriving an example relation from that seminal study. In addition, two trial constitutive relationships are constructed; these describe observations not well-modeled by *Ruina's* equations: lab tests of the unexpected weakening of silica-rich rocks of *Goldsby and Tullis* [2002] and geodetically observed periodic slow slip in the aseismic portion of subduction zones [*Dragert et al.*, 2004; *Ito et al.*, 2006].

1. Introduction

In laboratory faulting experiments where temperatures are less than a few hundred °C, slip rates are below a few mm/s, and total slip is limited to a few 100 μm , coseismic strength losses are typically less than 10% of the ambient stress (Figure 1a) [*Wong*, 1986] and the maximum slip velocity is proportional to the fault strength approximately by twice the ratio of the shear modulus to the shear wave speed (shear impedance) (Figure 1b) [e.g., *Johnson et al.*, 1973]. When these observations are extrapolated to natural conditions [e.g., *McGarr*, 1994; 1999; *McGarr and Fletcher*, 2003; *McGarr et al.*, 2004] they are consistent with typical natural earthquake properties: stress drops of a few tenths to a few MPa, low seismic efficiency, slip rates up to a few m/s and with rupture propagation at rates approaching the shear wave speed. The cause of the low seismic efficiency, small stress drops and high slip rates in laboratory faulting tests is a negative dependence of fault strength on the logarithm of slip velocity that is sustained over many orders of magnitude in velocity, typically from at least 0.001 $\mu\text{m/s}$ up to 0.75 mm/s at low normal stress and beyond 1 mm/s at higher stress [*Okubo and Dieterich*, 1986; *Kilgore et al.*, 1993], and that is second order relative to the ambient strength. The lab observations are well represented by rate and state variable constitutive equations [*Dieterich*, 1978; 1979; *Ruina*, 1983]. Though largely empirical, numerous advances in earthquake research have followed the development of these equations. Such work continues and these rate and state

relations are used routinely in models of the earthquake cycle, rupture propagation, triggered seismicity, time-dependent hazard, etc.

However, there are aspects of faulting that are not consistent with these particular rate and state equations. For example, in controlled laboratory tests at slip speeds up to 1 m/s [e.g., *Tsutsumi and Shimamoto, 1997; Goldsby and Tullis, 2002*], stress drops can be much larger (Figure 1a), having greater than 50% strength loss. These are thought to result from phase changes on the fault surface, not present in the low speed experiments on which the rate and state equations were based.

Another unrelated example is the periodic slow slip events (SSE) in subduction zones [*Dragert et al., 2004; Ito et al., 2006*]. SSE have stress drops that are small for earthquakes, extremely low average slip speeds in the range of 0.01 to 1 $\mu\text{m/s}$ (Figure 1b), and rupture propagation speeds of no more than a few meters per second. These properties are not consistent with rate weakening friction extending up to 1 mm/s as observed in typical stickslip faulting tests.

At near neutral steady-state rate dependence or at near critical stiffness, rate and state equations do allow for periodic slow slip [*Ruina, 1983; Lui and Rice, 2005*] and resonance phenomenon [*Perfettini et al., 2001, Lowry, 2006*]. While published modeling studies of SSE's find simulated events that are qualitatively similar to aspects of naturally observed slow slip events [*Lui and Rice, 2005; Lowry, 2006*], there are some concerns about attributing deep periodic phenomenon in subduction zones to rate and state friction effects without modification. These modeling studies use data consistent with the high temperature studies of *Blanpied et al. [1991; 1995]*, *Chester and Higgs [1992]*, and *Chester [1994; 1995]* who studied friction in the presence of water at temperatures up to 600°C. In the Blanpied study, steady-state rate dependence of granite was determined at 100 MPa water pressure and 400 MPa confining pressure. The Chester study involved stress relaxation tests at 100 MPa water pressure and 250 MPa confining pressure. Both studies show a broad range of temperatures where the rate dependence is measured or inferred to be negative, permitting frictional instability from >25° to 350°C for sliding velocities of 0.1 to 0.01 $\mu\text{m/s}$ (e.g., [*Blanpied et al., 1991*]). At higher temperatures, ductile processes such as solution transport creep (pressure solution) begin to affect the strength of load bearing contacts in the experimental fault zones [*Chester and Higgs, 1992*]. This high temperature regime shows strong velocity strengthening and stable sliding. While these experiments imply a seismic zone that corresponds roughly to natural observations, the sliding rates, corresponding to plate motion rates on natural faults, used in the steady-state sliding experiments are 10 to 100 times faster than typical plate rates. If the results of these studies are extrapolated in strain rate to an appropriate natural condition, the base of the seismogenic zone would occur at about 180°C for quartz and about 240°C for granite (see *Lockner and Beeler, 2000*). While these low temperatures are in reasonable agreement with the temperature at the base of the seismogenic zone for the Landers rupture, they are much less than the 350-400°C inferred for the San Andreas based on heat flow measurements [*Williams, 1996*].

Thus, while existing quartzofeldspathic experimental studies qualitatively predict many aspects of natural seismicity in strikeslip environments, the field observations are not matched closely. Of additional concern is, at the highest temperatures rate stepping tests in the lab studies indicate large departures from the typical rate and state form of *Ruina* [1983] (see *Blanpied et al.*, 1998).

Of greatest concern are the difference in composition and likely differences in stress, fluid pressure and temperature between the lab studies and the deep portion of subduction interfaces. Better knowledge of fault zone mineralogy, in situ effective normal stress and the rate dependence of more typical fault zone gouges (alteration products) at depth would be useful in providing more accurate representation of fault properties, particularly since in subduction zones fault strength appears to deviate significantly from that of quartzofeldspathic (Byerlee's law) materials.

Because high speed slip, SSEs, and other phenomenon such as deep non-volcanic tremor [*Obara*, 2002] and small repeating earthquakes [*Nadeau and Johnson*, 1998] are not easily represented by existing laboratory based constitutive equations, there is some need for new models of these and other poorly understood faulting phenomenon. In this report I describe an approach for constructing semi-empirical constitutive equations to represent laboratory or field observations. An objective is to follow *Ruina* [1983] and *Rice* [1983] to produce relatively simple relations that are slip- and time-differentiable, and that can be deployed in whole-cycle numerical earthquake models and calculations of rupture propagation. The equations are based on physical processes and contact scale physics where possible. In the case of field observations the approach is to use knowledge from related laboratory tests to further constrain the equations. In all cases, any 'state' variables will have a specific physical interpretation. In the following discussion I briefly summarize and contrast *Ruina's* and the new approach, re-derive a familiar state variable constitutive equation using the new approach, and then construct two new trial constitutive relationships. These new constitutive equations are for the unexpected weakening of silica-rich rocks observed by *Goldsby and Tullis* [2002] and for periodic slow slip in subduction zones [*Dragert et al.*, 2004; *Ito et al.*, 2006].

2. Background

Ruina's constitutive equations for low-temperature frictional sliding of rocks represent friction as the sum of a constant first-order value μ_0 , a second-order instantaneous dependence of friction on log velocity V and another second-order term containing a state variable ψ ,

$$\tau = \mu\sigma_e = \sigma_e \left(\mu_0 + a \ln \frac{V}{V_0} + b\psi \right).$$

Here and throughout τ is shear stress, σ_e is effective normal stress and friction is μ is the ratio of shear to normal stress. It assumed that the state variable is associated with a fault surface having a characteristic length scale d_c , and a dependence of strength on current slip speed and the

history of previous sliding. d_c is the sliding distance controlling the memory of prior sliding history. Ruina assumes that the change of state with time t is some function of state and slip rate V

$$\frac{d\psi}{dt} = G(\psi, V) \quad (1a)$$

The dependence of state on previous slip history is incorporated by requiring that strength depend on the displacement-weighted average w of some function f of slip speed

$$\psi = \int_{-\infty}^{\delta} w(\delta - \delta') f\left[\frac{V}{V_0}\right] d\delta'. \quad (1b)$$

Equation (1b) can satisfy (1a) and incorporate the characteristic length by allowing w to be an exponential decay over length d_c

$$\psi = \frac{1}{d_c} \int_{-\infty}^{\delta} \exp\left[-\frac{(\delta - \delta')}{d_c}\right] f\left[\frac{V}{V_0}\right] d\delta' \quad (2a)$$

Noting that (2a) can be expressed in the form of (1a) by differentiating,

$$\frac{d\psi}{dt} = \frac{V}{d_c} \left(f\left[\frac{V}{V_0}\right] - \psi \right) \quad (2b)$$

Ruina's [1980; 1983] equations for evolution of the state variable were constructed by choosing different functions for f . For example, taking f to be logarithmic produces an expression for the 'slip' state variable,

$$\frac{d\psi}{dt} = -\frac{V}{d_c} \left(\ln\left[\frac{V}{V_0}\right] + \psi \right). \quad (3)$$

Taking f to depend on $1/V$ yields an expression for the 'slowness' state variable.

While this approach was a breakthrough, leading to advances in modeling earthquake occurrence, it is likely that not all valuable state-variable relationships are of the form (1) and (2). For example, the evolution equation of *Perrin et al.* [1995] satisfies Ruina's condition equation (1a) but not equations (2), suggesting that (2) is too restrictive. A larger issue concerns the physical mechanisms that are attributed to state. As derived, Ruina's state variables intentionally were not attributed to physical mechanisms. Furthermore, when mechanisms are attributed to the equations, single state variables seem to represent more than one process. For instance, state in equations such as (3) is used to represent time-dependent strengthening observed at vanishingly low slip rates in laboratory tests. This effect had long been suspected to result from time-dependent yielding of asperity contacts [*Dieterich, 1972*], and direct observations of frictional surfaces have shown this to be the correct interpretation under particular circumstances [*Dieterich and Kilgore, 1994*]. At the same time, the same state variable also produces the apparent slip weakening which accompanies increases in sliding rate in rate-stepping experiments. This weakening seems to correspond to a 'brittle' behavior not easily or directly related to plastic yielding of asperities. State therefore could have the physical

interpretation of surface separation (dilation) as suggested by *Tolstoi* [1967] and as indicated by limited experimental observations [*Marone et al.*, 1990], or equivalently real area of contact, but may involve competition between time-dependent stress relaxation mechanisms that tend to increase area (decrease separation) and strain-dependent ones which reduce contact area (increase separation). In any case, without sound physical interpretation and a mechanistic basis, with associated material constants and activation energies, laboratory observations cannot be easily extrapolated to natural conditions and used in Earth models.

As a variation on *Ruina's*, the approach in this study is to assume that changes in fault strength depend on particular selected variables, such as slip, time, slip rate and shear stress, in the particular ways shown in laboratory tests. As an example, consider the familiar observations of rate dependent strength and slip weakening from low-temperature friction studies [*Dieterich*, 1972; 1978; 1979] as resulting from slip and rate dependences of a state variable that represents inelastic contacting area within the fault zone,

$$\psi = g(\delta, V) \quad \frac{d\psi}{dt} = \frac{\partial\psi}{dV} \frac{dV}{dt} + V \frac{\partial\psi}{d\delta}.$$

First, as noted in *Ruina* [1980], slip weakening following an increase in sliding velocity is nearly exponential so assume a strength change of that form, representing loss of contact area as

$$\frac{\partial\psi}{d\delta} = -\frac{\psi}{d_c} \quad \text{so that} \quad \frac{d\psi}{dt} = \frac{\partial\psi}{dV} \frac{dV}{dt} - \frac{V\psi}{d_c}.$$

The remaining right hand side term can be deduced by using the observational constraint that at steady state $\psi_{ss} = \ln(V_0/V)$

$$0 = \frac{\partial\psi}{dV} \frac{dV}{dt} - \frac{V}{d_c} \ln\left[\frac{V_0}{V}\right],$$

leading to *Ruina's* slip relation, equation (3)

$$\frac{d\psi}{dt} = -\frac{V}{d_c} \left(\ln\left[\frac{V}{V_0}\right] + \psi \right).$$

Both the slowness state evolution relation [*Ruina*, 1983] and *Perrin et al.'s* [1995] quadratic relationship can be deduced using combinations of laboratory constraints. And other useful state variable equations for low-temperature friction can also be constructed using this approach.

3. A trial constitutive relation for unexpected weakening.

As another example lab-derived constitutive relation, consider friction at higher sustained slip speed. For initially bare surfaces of silica-rich rocks (quartzite, novaculite, feldspar, and granite) at slips greater than a few meters at slip speeds from 10 mm to 0.1 m/s, there is a very large strength loss (Figure 1a, Figure 2a) [*Goldsby and Tullis*, 2002; *DiToro et al.*, 2004], whereas silica-poor rocks (gabbro) and silica-absent rocks (marble) show no weakening. Measurements and calculations indicate that asperity contact temperatures are <140 °C, and average temperatures on the sliding surface are 10's of degrees less than this, so melting is thought not to

be involved in the weakening [Goldsby and Tullis, 2002]. Furthermore, changes in strength occur more slowly than shear induced temperature changes on the fault surface so temperature does not directly influence shear strength. It has been proposed, on the basis of inference and microstructure observations, that shear lubricates the surface through production of a highly comminuted, comparatively wet, amorphous, gel-like material, i.e., “silica gel” [Goldsby and Tullis, 2002].

Interpretation of weakening. The primary observations of the weakened fault are well explained by a 'thixotropic' material [David Lockner ,personal communication], one whose strength is controlled by a near-fluid that becomes more fluid-like (weaker) when strained. In the case of a thixotropic gel, the weakening results from dynamic reduction of the number of chemical bonds between particles. Think of this as the progressive replacement of strong adhesive bonds between solid particles with weaker bonds. The transition from high friction at low-speeds to this unexpected weakening behavior at higher slip rates can be represented as a reduction of the number of active adhesive bonds in the gouge. When shearing ceases, or shearing rates are decreased, the material regains strength with time at a rate controlled by a chemical reaction that reforms the strong adhesive bonds. The net strength represents a dynamic balance between shear which decreases the number of strong bonds and time which increases their number. Therefore, we expect the steady state strength to decrease with increasing slip rate.

Some equations. Three constraints/assumptions are used to construct the fault strength relations:

(δ) Shearing produces a dynamic reduction of strong bonds.

(t) Time increases the number of strong bonds.

(ψ_{ss}) The steady-state number of strong bonds decreases with increasing slip speed.

Call the ratio of strong bonds to the total number of bonds state, ψ . Take μ_0 as the strength of the adhesive bonds, and μ_w as the lower strength of bonds within the gel. The combined macroscopic strength is

$$\tau = \mu\sigma_e = \sigma_e[(\mu_0 - \mu_w)\psi + \mu_w]. \quad (4)$$

Assume that state depends on slip and time, and allow an additional dependence that is initially unknown,

$$\psi = g(\delta, t, f) \quad \frac{d\psi}{dt} = \frac{\partial\psi}{\partial t} + V \frac{\partial\psi}{\partial\delta} + \frac{\partial\psi}{\partial f} \frac{df}{dt},$$

where f represents an undetermined variable or dependence. Based on lab observations and the expectation that shear is distributed within a layer of thickness w_c , we take the slip dependence at constant slip rate to be exponential with a characteristic distance d_c that scales with the layer thickness,

$$\frac{\partial\psi}{d\delta} = -\frac{\psi}{d_c} \text{ so that } \frac{d\psi}{dt} = \frac{\partial\psi}{\partial t} - \frac{V\psi}{d_c} + h.$$

where the unknown derivative product is replaced by h . By assuming that in the absence of slip the interparticle bonds are formed at a rate controlled by a chemical reaction, at constant temperature and zero slip rate the number of bonds increases with time. The first-order chemical reaction rate equation is exponential in time [Stumm and Morgan, 1981], $\psi = 1 - \exp(-t/t_c)$, where t_c is the reaction time constant, and the evolution equation becomes

$$\frac{\partial\psi}{\partial t} = \frac{1}{t_c}(1-\psi) \text{ so that } \frac{d\psi}{dt} = \frac{1}{t_c}(1-\psi) - \frac{V\psi}{d_c} + h$$

Trial forms for function h can be determined using the steady state strength as a constraint. In the lab tests strength decreases strongly with increasing velocity (Figure 2b) but these tests do not extend to high enough velocity to establish the complete form. In the absence of additional information, assume that there is no additional dependence, i.e., $h=0$. The steady value of state follows from setting both h and $d\psi/dt$ to zero in the expression immediately above, and

$$\frac{1}{\psi_{ss}} = \frac{t_c}{d_c} V_{ss} + 1.$$

Taking the ratio of displacement and time constants to be the characteristic velocity of the weakening process, $d_c/t_c=V_c$, the steady-state relation is

$$\psi_{ss} = \frac{V_c}{V_c + V_{ss}} \quad (5a)$$

Since the expectation is that the number of bonds decreases as the shear rate increases, the inverse relationship (5a) is adequate for the conceptual model and a decent representation of the data (Figure 2b). The evolution equation is simply

$$\frac{d\psi}{dt} = \frac{1}{t_c}(1-\psi) - \frac{V\psi}{d_c} = \frac{V_c}{d_c}(1-\psi) - \frac{V\psi}{d_c} \quad (5c)$$

At velocity $V \ll V_c$ the fault is strong $\mu = \mu_0$, and at $V \gg V_c$ the fault is weak at the residual strength $\mu = \mu_w$. V_c is the velocity at which the fault has lost half its strength, $\mu = (\mu_0 - \mu_w)/2$.

Discussion. Two simulations of rate steps using (4) and (5c) are shown in Figure 3. As the relation was constrained by the data, there is very good qualitative agreement with the observations, exponential shear weakening at high slip speed and rapid strength recovery when the loading rate reverts to values less than V_c . In addition, some predicted properties are consistent with the laboratory observations. For example, knowledge of the slip weakening distance ($d_c \approx 0.5$) and characteristic velocity ($V_c = 0.004$ m/s) result in a prediction for the characteristic time controlling the strength recovery. The prediction (121 s) is similar to the characteristic time of the observed recovery. Because (5) has a quasi-theoretical basis following a limited understanding of the underlying physics of the gel, additional implications can be tested in subsequent experiments, for example at higher slip rate where the relationship predicts constant strength or at higher temperature where the time constant of the reaction is expected to

decrease. One such prediction is evident in the simulations in Figure 3; the apparent slip weakening distance increases with increasing slip speed. In an iterative way, trial constitutive relations can be used to identify new experiments that will help to further constrain the underlying physics of weakening which in turn should lead to improved constitutive descriptions.

4. A trial constitutive relation for periodic slow slip.

Monitoring and increased instrument density above subduction zones in Japan and Cascadia have revealed episodic deformation thought to be due to fault slip but without much high frequency radiated energy: low frequency earthquakes, non-volcanic tremor, and slow slip events. The largest slow slip events in Cascadia have source dimensions consistent with large earthquakes, e.g., greater than 100 km, but source properties that are unlike large earthquakes: much longer durations of many days [Dragert *et al.*, 2004] and smaller total slip, typically a few centimeters.

Interpretation of slow slip. To derive a constitutive equation for modeling these observations, combine two observational constraints (denoted A and B below) and two laboratory constraints (C and D). At a constant rate of tectonic stress accumulation, the periodic nature of the slow slip events indicates slip at rates exceeding the average plate motion rate accompanies strength loss. The periodic nature also requires that the strength losses are followed by strength recovery at rates which initially exceed the tectonic stressing rate. In the rock mechanics literature such periodic faulting is called stickslip and has been modeled with lab-based constitutive equations that allow instability, such as rate and state friction. However in rate and state models of instability slip accelerates rapidly to high sliding velocities. That the recorded deformation of the largest of the slow events is at very low frequency suggests somewhat different source properties than in typical instability models - something prevents deformation at high strain rates. Here, the observed total slip and event duration are used to constrain the average slip velocity during the slow events. For instance, for slow slip events in Nankai Japan, the event duration (4.5×10^5 to 1×10^7 s) and total slip (0.017 to 0.11 m) imply average slip rates of 10 to 40 nm/s (1 to 4×10^{-8} m/s) [Ide *et al.*, 2007]. Frictional instability models accelerate to produce average slip velocities in the range of m/s [e.g., Rubin and Ampuero, 2005], which result when the fault is rate weakening, at least, in the range between the loading rate (typically on the order of 0.001 m/s) and the average slip rate (1 m/s). We therefore expect in the case of the slow slip events that the fault is (A) effectively rate weakening at the loading rate and above but (B) rate strengthening above the average slip speed.

These are properties of a brittle material that can experience a strength loss with accumulating inelastic shear strain through the typical dilatant mechanisms, but where the brittle behavior is partially suppressed or limited. Limits on strength loss are expected at these conditions and

perhaps even in the fully brittle regime. For instance, as described in Dieterich's original analysis, on which rate and state equations are based, the brittle component is a logarithmic dependence of strength on slip speed of the form

$$\mu = \mu_0 + B \log\left(\frac{V_0 + V}{V}\right)$$

[Dieterich, 1978]. Here V_0 is a 'cutoff' on strength loss when slip velocity greatly exceeds V_0 . That is, the fault can lose strength through reduction of contact area up to some limit. Such a limit was inferred to occur at low normal stress, even at room temperature for fault slip on granite surfaces [Okubo and Dieterich, 1986]. As temperature becomes more elevated at great depth, strength losses associated with brittle behavior become increasingly limited and eventually vanish at the brittle ductile transition [e.g., Evans et al., 1990; Evans and Kohlstedt, 1995].

The hypocentral depth of slow slip events (~35 km) and geotherm require source temperatures in excess of 450C. As plastic deformation is favored over brittle fault slip at low strain rate and high temperatures [e.g., Goetze and Evans, 1979], at these conditions the laboratory observations suggest that at the lowest slip speeds the fault is rate strengthening. So we require (C) rate strengthening at speeds below the loading rate. Laboratory observations also suggest hydrothermal processes can be important at these hypocentral conditions [Brantley et al., 1990]. So we expect (D) rapid strength recovery via hydrothermal processes such as crack healing and other lithification processes at the lowest slip rates.

Some equations. The constraints/assumptions used to construct the fault strength relations are: (δ) Shearing produces a dynamic reduction of contact area (shear weakening). The weakening is limited.

(t) Time allows for strength recovery (time strengthening) .

(V) The steady-state rate dependence is positive at sliding speed much lower than plate motion rate.

(V) The steady-state rate dependence is positive at sliding speed much higher than plate motion rate.

The limited brittle faulting model developed in this section is modified from the friction instability model of Dieterich [1978;1979], consisting of a first order fault strength μ_0 , a second order direct dependence on slip rate and a second order dependence on state:

$$\tau = \mu\sigma_e = \sigma_e\left(\mu_0 + a \ln \frac{V}{V_0} + c\psi\right). \quad (6)$$

The state variable ψ represents the inelastic portion of the shear load bearing surface area in the fault zone, in other words the portion of contacting area that can changes with slip and time,

$$\psi = g(\delta, t) \quad \frac{d\psi}{dt} = \frac{\partial\psi}{\partial t} + V \frac{\partial\psi}{\partial\delta}.$$

Take the slip dependence at constant slip rate to be typical slip weakening, exponential with a characteristic distance d_c ,

$$\frac{\partial \psi}{\partial \delta} = -\frac{\psi}{d_c} \text{ so that } \frac{d\psi}{dt} = \frac{\partial \psi}{\partial t} - \frac{V\psi}{d_c}.$$

During the interseismic period the fault regains strength by material transport processes such as crack healing and for simplicity I assume that these are rate limited by either the dissolution or precipitation step. Using the first-order chemical reaction rate equation [Rimstidt and Barnes, 1980] $\psi = 1 - \exp(-t/t_c)$, where t_c is the reaction time constant, and the evolution equation becomes

$$\frac{\partial \psi}{\partial t} = \frac{1}{t_c}(1 - \psi) \text{ so that } \frac{d\psi}{dt} = \frac{1}{t_c}(1 - \psi) - \frac{V\psi}{d_c}. \quad (7a)$$

Unlike (7a), in conventional state variable equations which have no 'cutoff' on rate and state effects [Ruina, 1983] strength recovery occurs with the passage of time or as slip velocity decreases and has no intrinsic limit. A consequential property of conventional state equations is the strength loss has no limit, being limited in simulations by other forces (inertia, radiation damping). As well as being consistent with hydrothermal reactions that might be reasonably expected at slow slip event hypocentral depths, the exponential healing function included in (7) produces the desired limit on state. That is, the fault can only recover to a value of $\psi=1$ and shear weakening can only reduce state to $\psi=0$ (Figure 4a). This limits the possible strength loss, and leads to an intrinsic bound on the slip speed during strength loss.

Equation (7a) can be rewritten

$$\frac{d\psi}{dt} = \frac{V_c}{d_c}(1 - \psi) - \frac{V\psi}{d_c} \quad (7b)$$

using the identity $V_c = d_c/t_c$. The steady state strength of (6) and (7) is

$$\mu = \mu_o + a \ln \frac{V}{V_c} + c \frac{V_c}{V_c + V} \quad (7c)$$

(Figure 4b). The steady-state rate dependence is

$$\frac{d\mu}{d \ln V} = a - c \frac{V/V_c}{(1 + V/V_c)^2} \quad (7d)$$

(Figure 4c). When strength is plotted against log velocity, the steady rate dependence is symmetric about V_c (Figure 4), and at V_c rate dependence is at its minimum. When $c/4 > a$ the rate dependence at V_c is negative and this is the necessary condition for strength loss.

Slider block simulations conducted with equations (6) and (7) show periodic stick-slip when elastic stiffness is significantly lower than $(c/4 - a)/d_c$. When V_c is sub micron/s, conditions are truly quasi-static at the highest slip speeds, and the 'slip' portion of the stick slip cycle can be simulated without consideration of inertia or radiation damping [e.g., Rice, 1993]. An example for loading rate $V_L = 0.001 \mu\text{m/s}$, stiffness $k = 2.76 \times 10^{-8} \text{ MPa}/\mu\text{m}$, and $V_c = 0.0033 \mu\text{m/s}$ is shown in Figure 5. The particular choice of the constitutive parameters a , c and σ_e (see

Discussion below) result in a rate weakening region between $5 \times 10^{-4} \mu\text{m/s}$ and $2.6 \times 10^{-2} \mu\text{m/s}$, a maximum slip speed of about $3 \mu\text{m/s}$, stress drop of 0.9 kPa , recurrence of 389 days, and event duration of 1.8 days.

Discussion. The parameter choices in the simulation (Figure 5) were made by fixing a to be similar to lab values for serpentine (see below), then selecting values of c and V_c to produce periodic slip at the imposed loading rate of 0.001 mm/s with maximum slip rate of the order of a micron/s. Having made these choices, to produce a stress drop on the order of 1 kPa , requires low effective normal stress relative to overburden at SSE hypocentral depth. While a careful and comprehensive study of parameter space has not been conducted it is likely that regardless of the particular friction model, the observations require very low effective stress, as follows. Approximately, a quasi-static frictional shear stress drop is the product of effective normal stress, the steady-state rate dependence and the logarithm of velocities,

$$\Delta\tau = \frac{d\mu}{d \ln V} \sigma_e \ln \frac{\hat{V}}{V_L}$$

where \hat{V} is the average slip velocity. If the stress drop is 1 to 10 kPa , and the velocity ratio is 10 to 1000 , the product $\sigma_e d\mu/d \ln V$ is 0.0044 to 0.00014 MPa . Noting that rate dependencies of considerably less than 0.001 can't be reliably measured experimentally, even if a rate dependence of 0.0001 is allowed the effective stress is 43 MPa , less than 7% of overburden minus hydrostatic fluid pressure at 35 km depth ($35 \text{ km} \times 18 \text{ MPa/km}$).

Qualitatively, the limited brittle behavior of (6) and (7) (Figure 4) resembles the rate dependence of serpentine at elevated temperature and pressure [Moore *et al.*, 1997] (Figure 6). As serpentine is a common mineral in subduction zones, its mechanical behavior is of some interest with regard to the properties of the slow slip events. Serpentine is well-known not to conform to simple rate and state friction, and is typically weaker than quartzofeldspathic rocks [Reinen *et al.*, 1994; Moore *et al.*, 1997]; the weakness may be a key to understanding the brittle response of serpentinite and other phyllosilicate phases [Escartin *et al.*, 1997].

In rock fracture tests anitigorite and lizardite serpentines are markedly weaker than non-hydrous silicate rocks such as granite and dunite and these serpentines have a lower dependence of failure stress on fault normal stress (pressure dependence). The difference in pressure dependence indicates low bulk dilatancy [see Brace *et al.*, 1966; Brace, 1978; Escartin *et al.*, 1997]. As serpentine has [001] cleavage, shear is accommodated preferentially along these cleavage surfaces resulting in crystallographically-controlled (non-opening) mode II shear fractures. Deformed serpentinite has scarce open mode I cracks that produce the strong pressure dependence in quartzofeldspathic rock. Dilatancy that does occur in serpentinite is restricted to rigid motion due to roughness along the shear planes [Escartin *et al.*, 1997] and in dilatant jogs within regions of shear step-over. For pre-existing faults, the analogous pressure dependence is the coefficient of friction μ . Assuming the same relation between pressure dependence and

dilatancy, comparison of μ of the typically strong quartzofeldspathic rocks with that of weak serpentines and other phyllosilicates suggests that dilatancy during frictional slip is similarly and relatively reduced for fault slip in phyllosilicate rich rocks.

Strength loss during rock failure or frictional slip requires net reduction of contacting area across the fault, which cannot occur unless dilatant volume is generated during the strength loss. So it is likely that at low slip rates where thermal effects are minimal, strength loss, like the pressure dependence of shear strength, is due to dilatancy, reflecting weakening due to shear induced reduction of contacting area across the fault surface. Any limits on brittle behavior, such as proposed in the construction of (7) are liable to be pronounced in the phyllosilicates.

Cautions. At present the constitutive relation (6) and (7) is a speculative description of friction at elevated temperature and pressure. Also, despite the arguments made above, the simulations shown in Figure 5 which resemble the gross character of natural slow slip do not use parameters derived from the chrysotile data shown in Figure 6. Furthermore, chrysotile is a low temperature serpentine variety and should not be present at the hypocentral depths of slow slip events. At room temperature, the response of the high temperature polymorph antigorite is not the same as chrysotile [Reinen *et al.*, 1994; Moore *et al.*, 1997] so Figure 5 should not be interpreted as resulting from an established fault rheology of serpentinite. Experiments on antigorite at hypocentral conditions have not been conducted and the existing data at lower temperatures and pressures extends only to sliding velocities of $0.1 \mu\text{m/s}$ rather than down to the rates shown in Figure 5 [Moore *et al.*, 1997] that are relevant to the slow events.

The relations (6) and (7) may not be a complete accounting of expected processes at SSE hypocentral conditions. If the fluid pressure in the crust were hydrostatic, at 450C the SSE source region would be either in the semi brittle or ductile regimes. In either event, based on rock fracture data stress drops could not occur [Evans *et al.*, 1990; Evans and Kohlstedt, 1995]. So, if it is reasonable to allow that fluid pressure is elevated enough, at least over a portion of the cycle, to allow brittle behavior, it is also reasonable to expect some component of ductile deformation in the near source region. A more complete fault model would allow the total deformation at the hypocentral depth to be partitioned between brittle strain and true ductile strain. The natural slow slip events account for only 2/3 of the plate motion at the source in Cascadia [Dragert *et al.*, 2004], consistent either with continuously accumulating elastic strain or with a non-brittle component of deformation being accommodated during the inter-event period. Neither of these possibilities are allowed by (6) and (7). The former explanation would seem to require that background stress in the hypocentral region is increasing quite significantly over the long term, requiring the fault strength of this region is increasing at the same rate. This could be incorporated in a fault model by allowing μ_0 in (6) to increase (linearly?) with time, although a physical motivation for allowing this is not immediately obvious. To account for the latter explanation, non-brittle components can be incorporated into fault zone models by introducing

strain-hardening prior to failure or a strain threshold for weakening and, to reiterate, such effects are expected at these depths. In nature such ductile strains may be very broadly distributed rather than associated with a 'fault'.

5. Conclusions

An approach to constructing constitutive equations for modeling seismic and aseismic faulting is described. It is a variation on *Ruina's* [1983] rate and state variable approach, but attributes physical meaning and identifies the particular processes associated with state. The intention is to use combine laboratory and field observations with theory and use all as constraints on the dependent variable derivatives of the state variable and on the steady-state values of state. The familiar state variable evolution equations developed by *Ruina* [1980, 1983] and widely used in earthquake modeling can be constructed using the alternative approach advocated here. The approach is demonstrated by applying it to two recent data sets that are not well modeled by the existing rate and state constitutive equations. In both of these cases, unexpected weakening of silica-rich rocks observed by *Goldsby and Tullis* [2002] and periodic slow slip in subduction zones [*Dragert et al.*, 2004; *Ito et al.*, 2006], the state variable has a simple interpretation and in both cases the state evolution equation combines exponential dependence on slip representing brittle (dilatant) shear weakening with an exponential dependence on time representing a chemical reaction that controls strength recovery.

6. References

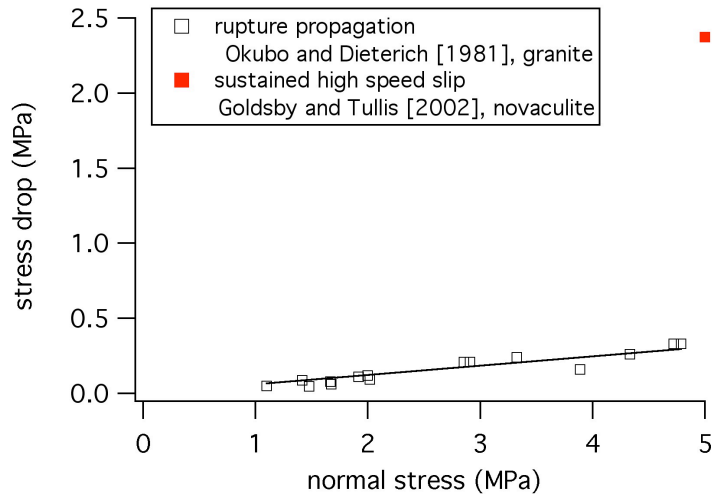
- Blanpied, M. L., D. A. Lockner, and J. D. Byerlee, Fault stability inferred from granite sliding experiments at hydrothermal conditions, *Geophys. Res. Lett.*, 18, 609-612, 1991.
- Blanpied, M. L., D. A. Lockner, and J. D. Byerlee, Frictional slip of granite at hydrothermal conditions, *J. Geophys. Res.*, 100, 13,045-13,064, 1995.
- Blanpied, M. L., C. J. Marone, D. A. Lockner, J. D. Byerlee, and D. P. King, Quantitative measure of the variation in fault rheology due to fluid-rock interactions, *J. Geophys. Res.*, 103, 9691-9712, 1998.
- Brace, W. F., Volume changes during fracture and frictional sliding, *Pure Appl. Geophys.*, 116, 603-614, 1978.
- Brace, W. F., B. W. Paulding, and C. H. Scholz, Dilatancy in the fracture of crystalline rock, *J. Geophys. Res.*, 71, 3939-3953, 1966.
- Brantley, S. L., B. Evans, S. H. Hickman, and D. A. Crerar (1990), Healing of microcracks in quartz: Implications for fluid flow, *Geology*, 18, 136– 139.
- Brune, J. N., Tectonic stress and the spectra of seismic shear waves from earthquakes, *J. Geophys. Res.*, 75, 4997-5009, 1970.
- Chester, F. M., Effects of temperature on friction: constitutive equations and experiments with quartz gouge, *J. Geophys. Res.*, 99, 7247-7262, 1994.

- Chester, F. M., A rheologic model for wet crust applied to strike-slip faults, *J. Geophys. Res.*, *100*, 13,033-13,044, 1995.
- Chester, F. M., and N. G. Higgs, Multimechanism friction constitutive model for ultrafine quartz gouge at hypocentral conditions, *J. Geophys. Res.*, *97*, 1859-1870, 1992.
- Dieterich, J.H., Time-dependent friction in rocks, *J. Geophys. Res.*, *77*, 3690-3697, 1972.
- Dieterich, J.H., Time-dependent friction and the mechanics of stick slip, *Pure Appl. Geophys.*, *116*, 790-806, 1978.
- Dieterich, J.H., Modeling of rock friction 1. Experimental results and constitutive equations, *J. Geophys. Res.*, *84*, 2161-2168, 1979.
- Dieterich, J.H. , and Kilgore, B.D., 1994, Direct observation of frictional contacts: New insights for sliding memory effects, *Pure Appl. Geophys.* *143*, 283-302.
- Dragert, H., K. Wang, and G. Rogers, Geodetic and seismic signatures of episodic tremor and slip in the northern Cascadia subduction zone, *Earth Planets Space*, *56*, 1143-1150, 2004.
- DiToro, G., D. L. Goldsby and T. E. Tullis, Friction falls towards zero in quartz rock as slip velocity approaches seismic rates, *Nature*, *47*, 436-439, 2004.
- Escartin, J., G. Hirth, and B. Evans, Nondilatant brittle deformation of serpentinites; implications for Mohr-Coulomb theory and the strength of faults, *J. Geophys. Res.*, *102*, 2897-2913, 1997.
- Evans, B., J. T. Fredrich, and T.-f. Wong (1990), The brittle-ductile transition in rocks: recent experimental and theoretical progress, in *Geophys. Monograph 56*, 1-21, AGU.
- Evans, B., and D. L. Kohlstedt, Rheology of rocks, in *Rock physics and phase relations*, AGU, 148-165, 1995.
- Goetze, C., and B. Evans (1979), Stress and temperature in the bending lithosphere as constrained by experimental rock mechanics, *Geophys. J. Roy. Astron. Soc.*, *59*, 463-478.
- Goldsby, D. L., and T. E. Tullis, Low frictional strength of quartz rocks at subseismic slip rates, *Geophys. Res. Lett.*, *29*, 4 pp, 2002.
- Ide, S., G. C. Beroza, D. R. Shelly and T. Uchide, A scaling law for slow earthquakes, *Nature*, *447*, 76-79, 2007.
- Ito, Y., K. Obara, K. Shiomi, S. Sekine, and H. Hirose, Slow earthquakes coincident with episodic tremors and slow slip events, *Science*, *26*, 503-506, 2006.
- Johnson, T. L., F. T. Wu, and C. H. Scholz, Source parameters for stick-slip and for earthquakes, *Science*, *129*, 278-280, 1973.
- Kilgore, B. D., M. L. Blanpied, and J. H. Dieterich, Velocity dependent friction of granite over a wide range of conditions, *Geophys. Res. Lett.*, *20*, 903-906, 1993.
- Liu, Y., and J. R. Rice, Aseismic slip transients emerge spontaneously in 3D rate and state modeling of subduction earthquake sequences, *J. Geophys. Res.*, *110*, B08307, doi:10.1029/2004JB003424, 2005.
- Lockner, D. A., and N. M. Beeler, Rock failure and earthquakes, in *International Handbook of Earthquake and Engineering Seismology* (Lee, Kanamori and Jennings eds.) 2002.

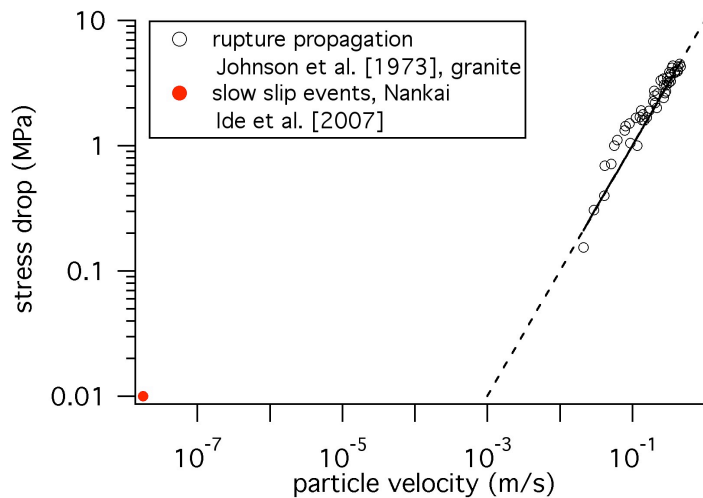
- Lowry, A. R., Resonant slow fault slip in subduction zones forced by climatic load stress, *Nature*, 442, 802-805, 2006.
- Marone, C., C. B. Raleigh, and C. H. Scholz, Frictional behavior and constitutive modeling of simulated fault gouge, *J. Geophys. Res.*, 95, 7007-7025, 1990.
- McGarr, A., Some comparisons between mining-induced and laboratory earthquakes, *Pure Appl. Geophys.*, 142, 467-489, 1994.
- McGarr, A., On relating apparent stress to the stress causing earthquake fault slip, *J. Geophys. Res.*, 104, 3003-3011, 1999.
- McGarr, A., and J. Fletcher, Maximum slip in earthquake fault zones, apparent stress, and stick-slip friction, *Bull. Seismol. Soc. Am.*, 93, 2355-2362, 2003.
- McGarr, A., J. Fletcher, and N. M. Beeler, Attempting to bridge the gap between laboratory and seismic estimates of fracture energy, *Geophys. Res. Lett.*, 31, 4pp, 2004.
- Moore, D.E., D.A. Lockner, S. Ma, R. Summers, and J.D. Byerlee (1997), Strengths of serpentinite gouges at elevated temperatures, *J. Geophys. Res.*, 102 (B7), 14,787-14,801.
- Nadeau, R. M. and L. R. Johnson, Seismological studies at Parkfield VI: Moment release rates and estimates of source parameters for small repeating earthquakes, *Bull. Seismo. Soc. Am.*, 88, 790-814, 1998.
- Obara, K., Nonvolcanic deep tremor associated with subduction in southwest Japan, *Science*, 296, 1679-1681, 2002.
- Okubo, P. G. and J. H. Dieterich (1981), Fracture energy of stick-slip events in a large scale biaxial experiment, *Geophys. Res. Lett.*, 8, 887-890.
- Okubo, P. G., and J. H. Dieterich, State variable fault constitutive relations for dynamic slip, In *Earthquake source mechanics*, ed. S. Das, J. Boatwright, and C. H. Scholz, *Geophys. Mono.* 37, AGU, 25-36, 1986.
- Perfettini, H., Schmittbuhl, J., Rice, J. R. & Cocco, M. Frictional response induced by time-dependent fluctuations of the normal loading. *J. Geophys. Res.* 106, 13455–13472, 2001.
- G. Perrin, J. R. Rice and G. Zheng, Self-healing Slip Pulse on a Frictional Surface, *Journal of the Mechanics and Physics of Solids*, 43, 1995, pp. 1461-1495, 1995.
- Rice, J. R. (1983), Constitutive relations for fault slip and earthquake instabilities, *Pure Appl. Geophys.*, 121, 443-475.
- Rice, J. R. (1993), Spatio-temporal complexity of slip on a fault, *J. Geophys. Res.*, 98, 9885-9907.
- Reinen, L. A., J. D. Weeks, and T. E. Tullis (1994), The frictional behavior of lizardite and antigorite serpentinites: Experiments, constitutive models, and implications for natural faults, *Pure and Appl. Geophys.*, 143, 317-358.
- Rimstidt, J. D. and H. L. Barnes, The kinetics of silica-water reactions, *Geochimica et Cosmochimica Acta*, 44, 1683-1699, 1980

- Rubin, A.M., and J.-P. Ampuero, Earthquake nucleation on (aging) rate-and-state faults, *J. Geophys. Res.*, VOL. 110, B11312, doi:10.1029/2005JB003686, 2005
- Ruina, A. L. (1980). Friction laws and instabilities, a quasistatic analysis of some dry frictional behavior, PhD Thesis, Brown University, 99 pp.
- Ruina, A. L., Slip instability and state variable friction laws, *J. Geophys. Res.*, 88, 10359-10370, 1983.
- Stumm, W., and J. J. Morgan, *Aquatic chemistry*, John Wiley and Sons, New York, 780p., 1981.
- Tolstoi, D. M. (1967). Significance of the normal degree of freedom and natural normal vibrations in contact friction, *Wear*, 10, 199-213.
- Tsutsumi, A., and T. Shimamoto, High-velocity frictional properties of gabbro, *Geophys. Res. Lett.*, 24, 699-702, 1997.
- Williams, C. F., Temperature and the seismic/aseismic transition: Observations from the 1992 Landers earthquake, *Geophys. Res. Lett.*, 23, 2029-2032, 1996.
- Wong, T.-f., On the normal stress dependence of the shear fracture energy, in *Earthquake Source Mechanics*, *Geophys. Monogr. Ser.*, Vol. 37, edited by S. Das et al., pp. 1-11, AGU, Washington, D.C., 1986.

Figures



a)



b)

Figure 1. Source properties from rupture propagation experiments. a) Variation of strength loss, with normal stress during slip between granite surfaces from *Okubo and Dieterich* [1981] (open symbols). The line is a fit constrained to pass through (0,0) with resulting slope 0.06 MPa/MPa. Also shown is data from sustained slip at high speed on novaculite (red) from *Goldsby and Tullis* [2002]. b) Variation of peak near fault particle velocity with strength loss during rupture propagation between granite surfaces from *Johnson et al.*, [1973]. Line is the expression of *Brune* [1970] relating stress drop $\Delta\tau$ to particle velocity \dot{u} , $\Delta\tau = G\dot{u}/\beta$, with $G=30,000$ MPa and $\beta=3000$ m/s. Also shown is typical source properties of slow slip events in Nankai, Japan (red). Particle velocity is taken as half the ratio of average slip (0.016 m) to average event duration (4.5×10^5 s) [*Ide et al.*, 2007, Table 1] and the strength loss is 10 kPa [*Ide et al.*, 2007].

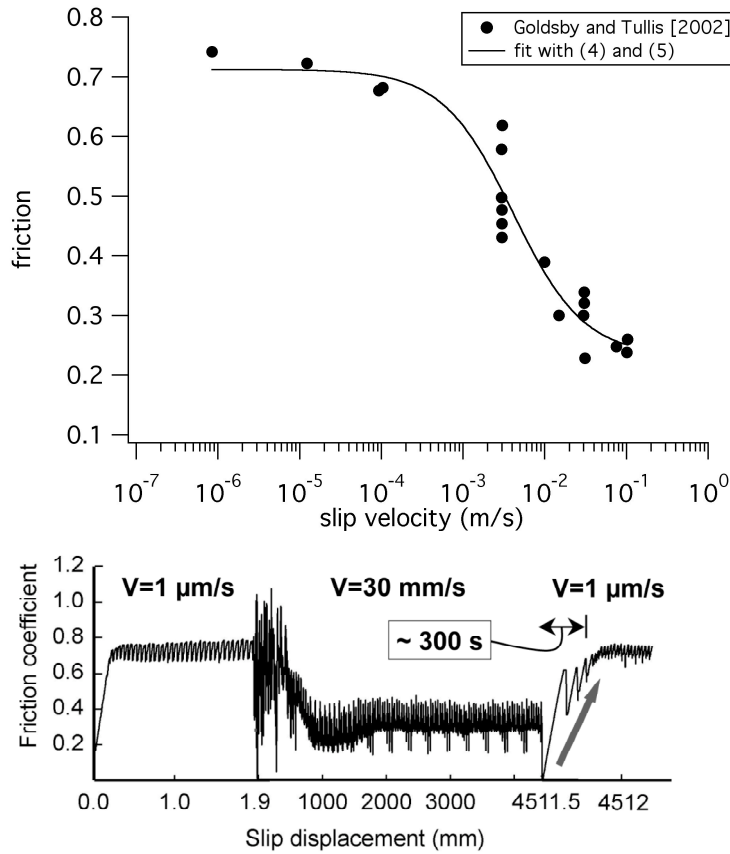


Figure 2. Unexpected and extraordinary rate weakening. a) *Goldsby and Tullis* [2002] data from novaculite at 5 MPa normal stress showing the dependence of steady-state friction on slip rate. Shown for reference is a fit to the data using equations (4) and (5), resulting in $\mu_0=0.71$, $\mu_w=0.23$, and $V_c=0.0041$ m/s. b) Summary of strength loss and strength recovery due to unexpected weakening of novaculite. Friction with slip at 1 $\mu\text{m/s}$, 30 mm/s, and again at 1 $\mu\text{m/s}$. Note the scale of the horizontal axis changes with velocity [*DiToro et al.*, 2004].

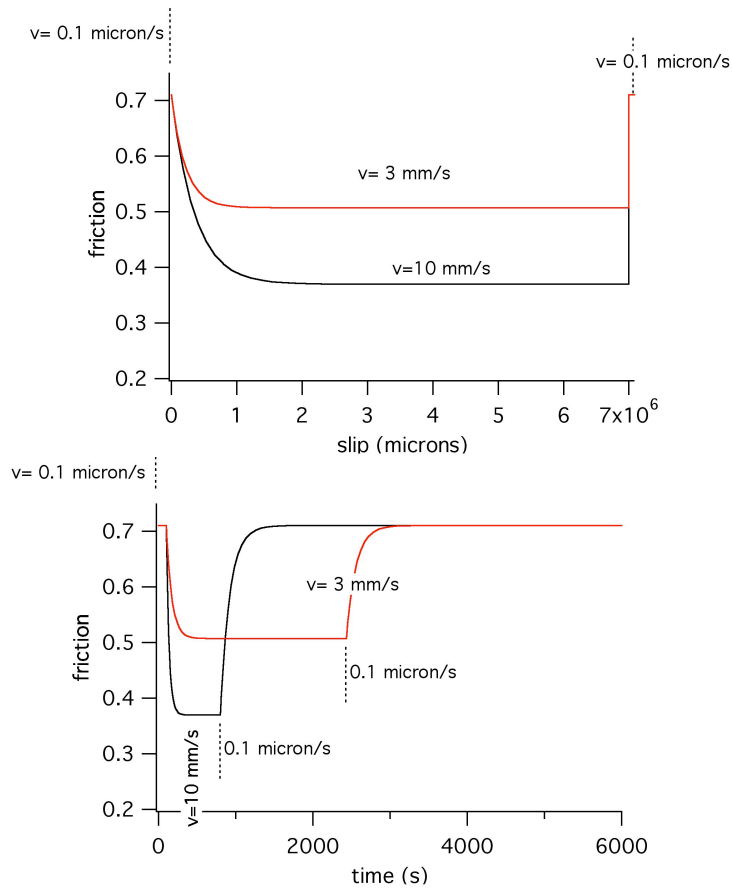


Figure 3. Simulations of unexpected weakening using step increases and decreases in sliding velocity for two different sized rate steps (0.1 microns/s to 3 mm/s, 0.1 microns/s to 10 mm/s) in friction vs displacement and friction vs time with equations (4) and (5). The simulation steps down after slip of 10 microns, then back up after slip of 7 meters, $d_c = 0.5$ m, $t_c = 121$ s, $\mu_0 = 0.71$, $\mu_w = 0.23$, and $V_c = 4.1$ mm/s.

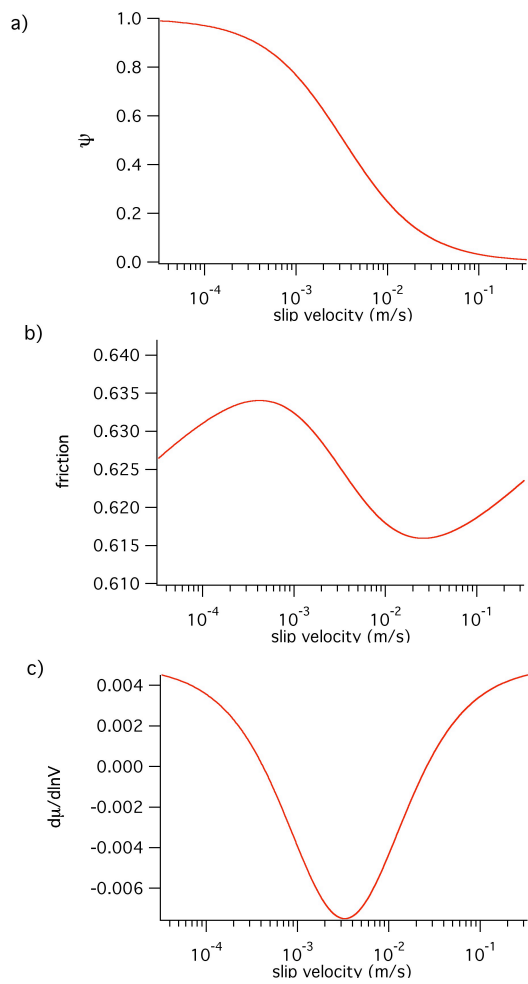
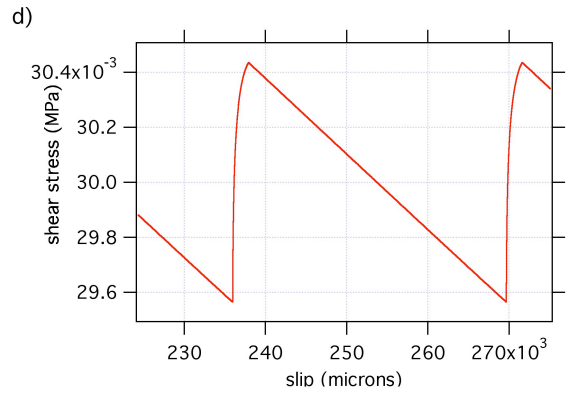
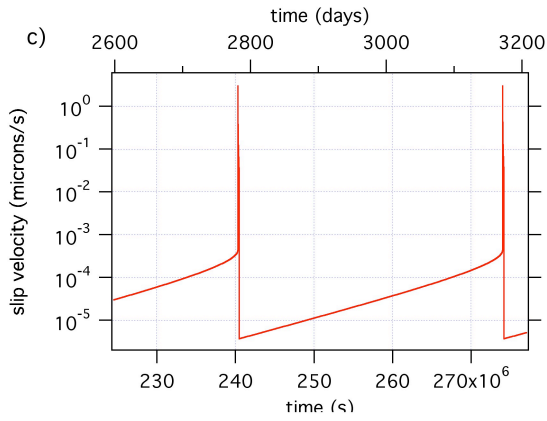
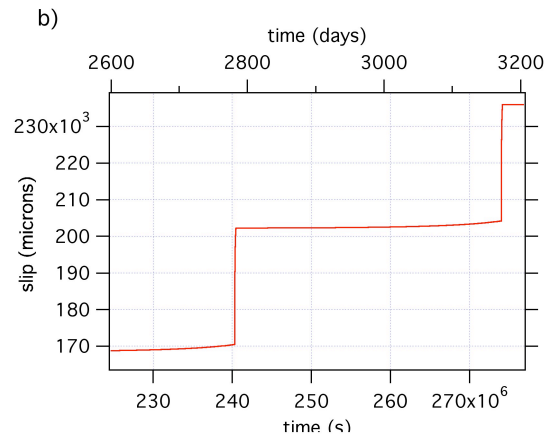
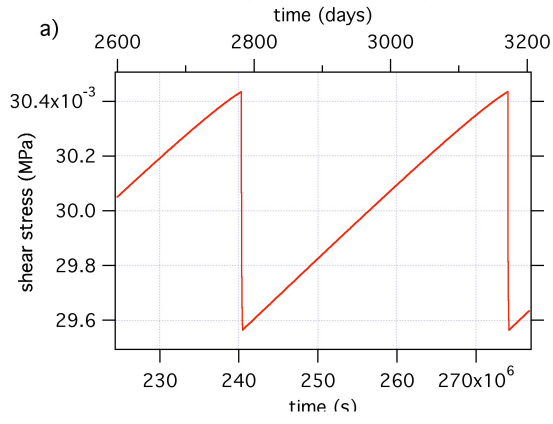


Figure 4. Steady state properties of constitutive relation for periodic slow slip, equations (6) and (7) with $a=0.005$, $c=0.05$, $V_c= 0.0033 \mu\text{m/s}$. a) State. b) Strength c) Rate dependence.

1d model of periodic slow slip



1d model of periodic slow slip

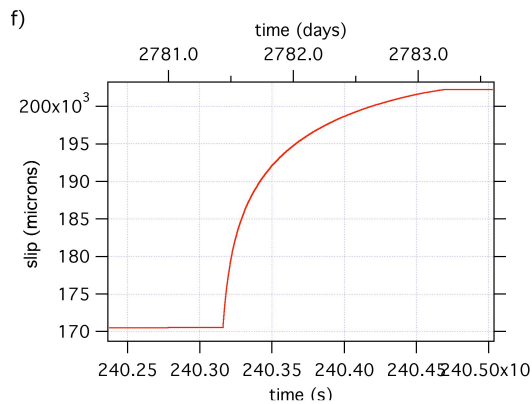
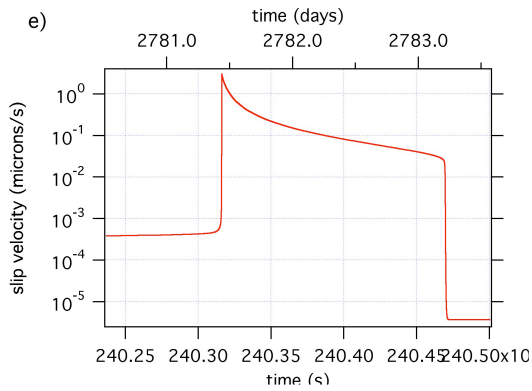


Figure 5. Numerical simulation of equations (6) and (7) with a single degree of freedom slider block. For quasi-static conditions the equation of block motion reduces to $d\tau/dt = k(V_L - V)$ where k is the elastic stiffness and V_L is the load point velocity. In this simulation $V_L = 0.001 \mu\text{m/s}$, $k = 2.76 \times 10^{-8} \text{ MPa}/\mu\text{m}$, $V_c = 0.0033 \mu\text{m/s}$, $\mu_0 = 0.6$, $a = 0.005$, $c = 0.05$ and $\sigma_n = 48 \text{ kPa}$ (0.048 MPa). a) Shear stress vs time. b) Slip vs time. c) Slip velocity vs time. d) Shear stress vs slip. e) Detailed view of slip velocity during 'rapid' slip event. f) Detailed view of slip during 'rapid' slip event.

serpentine - Moore et al. [1997]

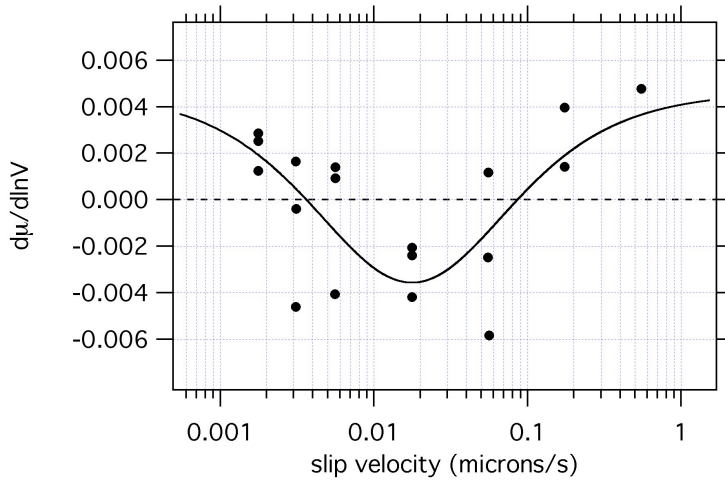


Figure 6. Variation of the steady state rate dependence of chrysotile serpentine with sliding velocity at temperatures between 107 and 281 °C and effective normal stresses between 46.5 and 139.5 MPa, from *Moore et al.*, 1997. The conditions are consistent with those at depths between 3 and 9 km in the crust assuming hydrostatic pore fluid pressure and normal stress equal to overburden. Shown also is a fit to this data using equation (7d) resulting in $a = 0.0046$, $c = 0.032$ and $V_c = 0.018 \mu\text{m/s}$.